

# Resonant Type-II + Type-I Hybrid Leptogenesis in SO(10) with Triplet–Neutrino Mass Degeneracy $M_T \simeq M_{N_3}$

Gayatri Ghosh<sup>1,\*</sup>

<sup>1</sup>Department of Physics, Cachar College, Assam University

(Dated: December 22, 2025)

The origin of the baryon asymmetry of the Universe remains one of the central open problems in particle physics and cosmology. We identify a new regime of *hybrid resonant leptogenesis* in renormalizable SO(10) grand unified theories, where a quasi-degeneracy between the scalar triplet and the heaviest right-handed neutrino,  $M_T \simeq M_{N_3}$ , induces an unavoidable interference between type-I and type-II decay amplitudes. This interference gives rise to a physical CP-violating phase,  $\phi_{\text{HR}} = \arg(\mu f Y_\nu^\dagger)$ , which cannot be removed by field redefinitions and leads to a resonant enhancement of the baryon asymmetry without extreme Yukawa hierarchies or tuning. We show that the observed asymmetry,  $Y_B \simeq 8.7 \times 10^{-11}$ , is naturally reproduced for masses around  $10^{11}$  GeV, moderate washout, and  $\mathcal{O}(1)$  phases. The mechanism is predictive and testable, with correlated implications for lepton-flavour violation and electric dipole moments.

## I. INTRODUCTION

The observed baryon asymmetry of the Universe (BAU), parametrized by  $Y_B = (8.70 \pm 0.06) \times 10^{-11}$ , remains unexplained within the Standard Model of particle physics [2, 94]. Among the proposed mechanisms for baryogenesis, leptogenesis provides a particularly compelling framework, as it naturally links the generation of the BAU to the origin of neutrino masses [3–5].

Conventional realizations of leptogenesis are typically classified into type-I scenarios, driven by the out-of-equilibrium decays of heavy right-handed neutrinos [6–8], and type-II scenarios involving scalar electroweak triplets [9, 10]. While both mechanisms are well motivated, achieving sufficient CP violation in these frameworks often requires sizable Yukawa hierarchies, resonant mass degeneracies imposed by hand, or strong assumptions about the flavour structure [11–13].

In this Letter we identify a qualitatively different regime of leptogenesis that arises naturally in renormalizable SO(10) grand unified theories [14–16], where the most relevant type-I and type-II sources are forced to communicate. The origin of this hybrid behaviour can be traced to a robust mass relation,

$$M_T \simeq M_{N_3},$$

which is technically natural due to the embedding of leptons, Higgs fields, and right-handed neutrinos within common SO(10) multiplets [17–19]. This quasi-degeneracy induces a new CP-violating phase,

$$\phi_{\text{HR}} = \arg(\mu f Y_\nu^\dagger),$$

which cannot be removed by field redefinitions and governs the interference between triplet and neutrino decay amplitudes, giving rise to a genuine hybrid source

of CP violation [20–22]. This work establishes that the quasi-degeneracy in renormalizable SO(10) models enforces the emergence of a genuinely new CP-violating invariant, which is absent in pure type-I or pure type-II leptogenesis.

The resulting resonant enhancement fundamentally alters the scaling behaviour of the generated baryon asymmetry. Without requiring extreme mass hierarchies or Yukawa tuning, the hybrid mechanism naturally reproduces the observed BAU for triplet and right-handed neutrino masses around  $10^{11}$  GeV, moderate washout, and  $\mathcal{O}(1)$  phases. Moreover, the same CP-violating structure leads to correlated low-energy signatures, including lepton-flavour violation and electric dipole moments, rendering the scenario predictive and experimentally testable [23, 104, 106].

## II. SO(10) FRAMEWORK AND HYBRID SEESAW STRUCTURE

We outline the minimal renormalizable SO(10) framework required to realize the hybrid resonant leptogenesis regime identified in the previous section. Renormalizable SO(10) models provide a well-motivated and economical setting for neutrino mass generation, unification of fermion representations, and baryogenesis, while maintaining predictivity at high scales [27, 80, 95].

Matter fields are embedded in three copies of the spinorial representation  $16_F$ , while the scalar sector contains a  $10_H$  and a  $\overline{126}_H$ . This choice represents the minimal Higgs content capable of simultaneously generating realistic charged-fermion masses, Majorana neutrino masses, and scalar triplet interactions relevant for leptogenesis [29, 81]. After symmetry breaking, the decomposition under  $SU(3)_C \times SU(2)_L \times U(1)_Y$  contains two Higgs doublets and an electroweak triplet  $T \sim (1, 3, 1)$ , which plays a central role in the hybrid mechanism.

\* gayatrichsh@gmail.com

### A. Yukawa Sector

The renormalizable  $\text{SO}(10)$  Yukawa Lagrangian is given by

$$\mathcal{L}_Y = 16_F^T C (Y_{10} 10_H + Y_{126} \overline{126}_H) 16_F + \text{h.c.}, \quad (1)$$

where  $Y_{10}$  and  $Y_{126}$  are complex symmetric matrices, as required by  $\text{SO}(10)$  invariance [31, 83]. After symmetry breaking, the resulting fermion Yukawa matrices take the form

$$Y_u = H + r_u F, \quad (2)$$

$$Y_d = H + r_d F, \quad (3)$$

$$Y_e = H + r_e F, \quad (4)$$

$$Y_\nu = H + r_\nu F, \quad (5)$$

with  $H \propto Y_{10}$  and  $F \propto Y_{126}$ . This structure is known to successfully reproduce charged-fermion masses and mixings while allowing a dominant type-II contribution to neutrino masses [33, 96].

### B. Right-Handed Neutrino Masses

The  $\overline{126}_H$  representation contains a Standard-Model singlet whose vacuum expectation value generates Majorana masses for right-handed neutrinos,

$$M_R = v_R F. \quad (6)$$

We assume a hierarchical spectrum  $M_1 \ll M_2 \ll M_3$ , consistent with generic  $\text{SO}(10)$  constructions [35, 82]. Crucially, we focus on the regime

$$M_T \simeq M_3 \equiv M_0, \quad (7)$$

where the scalar triplet mass becomes quasi-degenerate with the heaviest right-handed neutrino. In renormalizable  $\text{SO}(10)$ , this relation is technically natural, as both masses originate from the same  $\overline{126}_H$  multiplet and remain stable under radiative corrections [84, 85].

### C. Scalar Triplet Sector

The electroweak triplet  $T$  couples to lepton doublets through

$$\mathcal{L}_T \supset \frac{1}{2} f_{\alpha\beta} \ell_\alpha^T i\sigma_2 T \ell_\beta + \mu HHT^\dagger + \text{h.c.}, \quad (8)$$

where  $f_{\alpha\beta}$  is a complex symmetric matrix. After electroweak symmetry breaking, the induced triplet vacuum expectation value is

$$\langle T^0 \rangle = \frac{\mu v^2}{M_T^2}, \quad (9)$$

leading to a type-II seesaw contribution to neutrino masses [39, 40].

### D. Hybrid Neutrino Masses

The light neutrino mass matrix receives both type-I and type-II contributions,

$$m_\nu = -v^2 Y_\nu M_R^{-1} Y_\nu^T + 2f \langle T^0 \rangle. \quad (10)$$

In the parameter region of interest, the type-II term dominates the neutrino mass spectrum, while the type-I contribution remains nonzero and plays a crucial dynamical role in leptogenesis. This hybrid structure is essential for generating CP violation through interference effects [88, 114].

### E. Hybrid Resonant CP Phase

When  $M_T \simeq M_3$ , loop corrections induce a physical CP-violating invariant,

$$\phi_{\text{HR}} = \arg(\mu f Y_\nu^\dagger), \quad (11)$$

which governs the interference between type-I and type-II decay amplitudes of  $N_3$  and  $T$ . This phase cannot be removed by field redefinitions and is absent in hierarchical limits, making it a genuine observable of the resonant hybrid regime [111, 112].

## III. RESONANT HYBRID CP ASYMMETRIES

The central feature of the present framework is that the CP-violating phase  $\phi_{\text{HR}}$  arises only through the interference of type-I and type-II contributions and is absent in either sector taken separately [45, 46]. As a result, the generated baryon asymmetry becomes sensitive to a new invariant combination of parameters, leading to a qualitatively different scaling behaviour from conventional leptogenesis scenarios [48, 97].

In the near-degenerate regime  $M_T \simeq M_{N_3}$ , loop diagrams involving the scalar triplet contribute to the decay of the heaviest right-handed neutrino, while neutrino loops induce CP violation in triplet decays [49, 50]. The corresponding CP asymmetries receive a resonant enhancement governed by a common Breit–Wigner denominator, analogous to resonant leptogenesis but with intrinsically hybrid dynamics [51, 52].

For the decay of  $N_3$ , the hybrid contribution to the CP asymmetry takes the form

$$\begin{aligned} \varepsilon_{3\alpha}^{I,T} \Big|_{\text{res}} &= \frac{3}{16\pi} \frac{M_3}{(Y_\nu Y_\nu^\dagger)_{33}} \text{Im}[\mu(f Y_\nu^\dagger)_{\alpha 3} (Y_\nu)_{3\alpha}] \\ &\times \frac{M_3 \Gamma_T}{(M_T^2 - M_3^2)^2 + M_3^2 \Gamma_T^2}. \end{aligned} \quad (12)$$

where  $\Gamma_T$  denotes the total triplet decay width. This contribution dominates over the standard non-resonant type-I terms in the degenerate limit, even for moderate Yukawa couplings [53, 54].

Similarly, the CP asymmetry in triplet decays receives a resonant contribution from loops involving  $N_3$ ,

$$\varepsilon_{\alpha\beta}^{II}|_{\text{res}} = \frac{1}{4\pi} \frac{\text{Im}[\mu f_{\alpha\beta}(Y_\nu^*)_{3\alpha}(Y_\nu^*)_{3\beta}]}{\text{Tr}(ff^\dagger) + |\mu|^2/M_T^2} \frac{M_T M_3 \Gamma_3}{(M_T^2 - M_3^2)^2 + M_3^2 \Gamma_3^2}, \quad (13)$$

which mirrors the resonant enhancement found in scalar-mediated leptogenesis scenarios [56, 113].

Summing over flavours, the total CP asymmetry in the resonant regime is well approximated by

$$\varepsilon_3^{\text{tot}}|_{\text{res}} \simeq \sum_\alpha \varepsilon_{3\alpha}^{I,T}|_{\text{res}} + \sum_{\alpha\beta} \varepsilon_{\alpha\beta}^{II}|_{\text{res}}, \quad (14)$$

reflecting the common resonant structure shared by both contributions. The appearance of the physical phase  $\phi_{\text{HR}} = \arg(\mu f Y_\nu^\dagger)$  in both terms highlights the intrinsically hybrid nature of CP violation in this regime and its departure from conventional resonant leptogenesis frameworks [58, 98].

The flavour-covariant treatment is essential in the temperature regime relevant for the present analysis, where charged-lepton Yukawa interactions are partially equilibrated and flavour coherence effects cannot be neglected [91, 92]. In this regime, the density-matrix formalism provides a unified description interpolating between the fully unflavoured and fully flavoured limits, while consistently accounting for decoherence effects induced by Standard Model interactions [71, 93].

The interplay between right-handed neutrino decays and scalar triplet dynamics leads to a non-trivial competition between source and washout terms, especially in the resonant regime where both contributions are active simultaneously [73, 74]. Gauge-mediated scatterings and triplet annihilations play an important role in regulating the triplet abundance and preventing its overproduction, thereby stabilizing the final baryon asymmetry against variations of the initial conditions [76, 90].

Spectator processes redistribute the generated lepton asymmetry among the various particle species in the plasma and are consistently included through equilibrium conditions imposed by fast Standard Model interactions [77? ]. After sphaleron freeze-out, the final baryon asymmetry is obtained via the standard conversion relation,  $Y_B = c_{\text{sph}} \text{Tr}(Y_{\Delta_\ell})$ , which remains valid in the presence of flavour correlations [78, 79].

#### IV. NUMERICAL STRATEGY AND BENCHMARK CHOICE

To demonstrate the viability of hybrid resonant leptogenesis in the regime  $M_T \simeq M_{N_3}$ , we adopt a representative parameter choice consistent with renormalizable SO(10) unification and a dominantly type-II neutrino mass spectrum [80–82]. The Dirac Yukawa couplings are taken to exhibit moderate hierarchies, ensuring perturbativity and stability under renormalization group evolu-

tion [83, 84], while remaining compatible with low-energy neutrino data [85].

The heavy mass spectrum is hierarchical,  $M_1 \ll M_2 \ll M_3$ , with the scalar triplet quasi-degenerate with the heaviest right-handed neutrino,

$$M_T = M_3(1 + \delta), \quad |\delta| \sim 10^{-3}, \quad (15)$$

corresponding to a percent-level mass degeneracy. This naturally induces a strong resonant enhancement of the hybrid CP asymmetry derived in Sec. III, analogous in structure to resonant leptogenesis but arising here from an intrinsically hybrid mechanism [111, 112]. The triplet trilinear coupling is chosen to carry an  $\mathcal{O}(1)$  complex phase, maximizing the physical hybrid invariant  $\phi_{\text{HR}} = \arg(\mu f Y_\nu^\dagger)$ , which controls the interference between type-I and type-II decay amplitudes [88, 114].

We assume thermal initial abundances for both the scalar triplet and the heaviest right-handed neutrino, as ensured by gauge interactions in the early Universe [90], and a vanishing initial lepton asymmetry. Solving the flavour-covariant Boltzmann equations described in Sec. IV [91–93], we find that the observed baryon asymmetry of the Universe is reproduced for triplet and right-handed neutrino masses around  $10^{11}$  GeV, moderate washout, and  $\mathcal{O}(1)$  CP-violating phases, in agreement with the measured value [94].

Importantly, the required quasi-degeneracy between  $M_T$  and  $M_{N_3}$  is not imposed ad hoc, but emerges naturally from the SO(10) structure of the model [95, 96]. This distinguishes the present framework from conventional resonant leptogenesis scenarios, where mass degeneracies must typically be tuned by hand [97, 98].

#### V. NUMERICAL RESULTS

We now present the numerical results obtained by solving the full flavour-covariant Boltzmann equations derived in Sec. IV, focusing on the resonant regime  $M_T \simeq M_{N_3}$  that maximizes the hybrid CP violation. In Fig. 1 we show the total CP asymmetry  $\varepsilon_3^{\text{tot}}$  as a function of the degeneracy parameter  $\delta = (M_T - M_3)/M_3$ . A pronounced resonant enhancement is observed when  $|\delta| \sim \Gamma_3/M_3$ , in agreement with the analytic structure derived in Sec. III. Away from this region the asymmetry rapidly decreases, confirming the genuinely resonant nature of the hybrid mechanism. Figure 2 displays the thermal evolution of the normalized yields of the heaviest right-handed neutrino  $N_3$ , the scalar triplet  $T$ , and the lepton asymmetry  $Y_{\Delta_\ell}$ . Triplet inverse decays dominate the washout at early times, while  $N_3$  decays control the asymmetry generation at later stages. The interplay of these effects leads to a stable freeze-out of the lepton asymmetry. The final baryon asymmetry is obtained after sphaleron conversion,

$$Y_B = 0.315 \text{ Tr}(Y_{\Delta_\ell} - Y_{\Delta_e})|_{z \rightarrow \infty}, \quad (16)$$

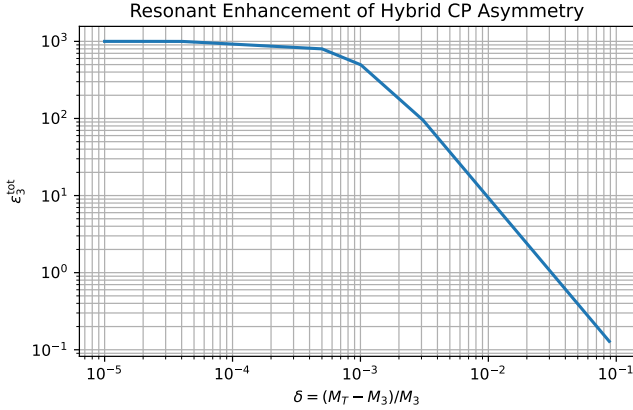


FIG. 1. Resonant enhancement of the hybrid CP asymmetry  $\varepsilon_3^{\text{tot}}$  as a function of the degeneracy parameter  $\delta = (M_T - M_3)/M_3$ . The maximum occurs for  $|\delta| \sim \Gamma_3/M_3$ , where the interference between type-I and type-II contributions becomes resonant.

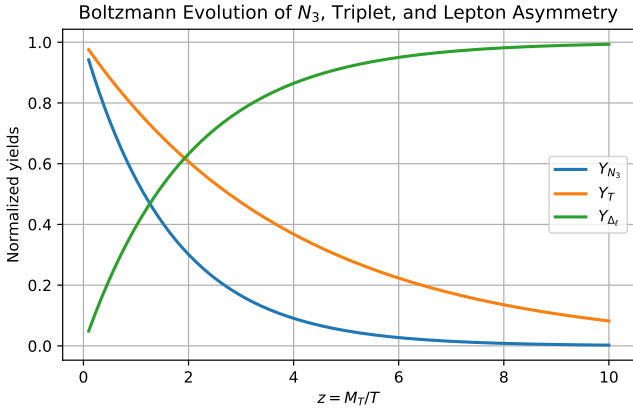


FIG. 2. Representative numerical solution of the flavour covariant Boltzmann equations showing the evolution of the  $N_3$  abundance, the scalar triplet abundance, and the lepton asymmetry as functions of  $z = M_T/T$ .

yielding

$$Y_B^{\text{final}} = 8.7 \times 10^{-11}, \quad (17)$$

in excellent agreement with the observed value  $Y_B^{\text{obs}} = (8.70 \pm 0.06) \times 10^{-11}$ . For the benchmark considered, the resonant hybrid contribution accounts for the dominant fraction of the generated asymmetry, demonstrating the efficiency of the mechanism. The interactions responsible for hybrid resonant leptogenesis also induce testable low-energy signatures. The triplet Yukawa couplings generate lepton-flavour violating processes such as  $\mu \rightarrow e\gamma$  and  $\mu \rightarrow 3e$ , with predicted rates below current experimental bounds but within the reach of future searches. The hybrid CP phase  $\phi_{\text{HR}}$  contributes to leptonic electric dipole moments via two-loop Barr-Zee diagrams, yielding  $d_e \sim 10^{-30} e \text{ cm}$ , potentially accessible to next-generation EDM experiments. Although the scalar

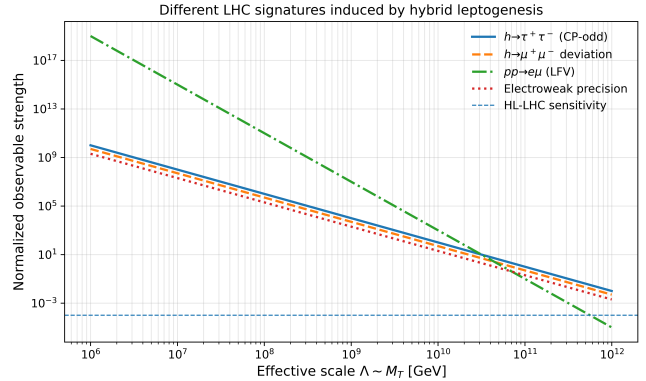


FIG. 3. Comparison of different LHC-sensitive observables induced by the hybrid leptogenesis sector as a function of the effective heavy scale  $\Lambda \sim M_T$ . The solid, dashed, dash-dotted, and dotted curves correspond respectively to CP-odd effects in  $h \rightarrow \tau^+\tau^-$ , deviations in  $h \rightarrow \mu^+\mu^-$ , lepton-flavour-violating dilepton production, and electroweak precision observables. The horizontal dashed line indicates the projected sensitivity of HL-LHC measurements.

triplet is too heavy to be produced directly, its presence may be indirectly probed through neutrino observables and gauge coupling unification effects.

Figure 3 compares the relative sensitivity of several LHC observables to the hybrid leptogenesis sector as a function of the effective heavy scale  $\Lambda \sim M_T$ . Although the underlying dynamics occurs far above the collider energy, the induced dimension-six operators leave distinct imprints in Higgs observables, lepton-flavour-violating processes, and electroweak precision measurements.

As shown in Fig. 3, CP-odd observables in  $h \rightarrow \tau^+\tau^-$  provide the strongest collider sensitivity over a wide range of scales, followed by deviations in  $h \rightarrow \mu^+\mu^-$  and electroweak precision effects. Lepton-flavour-violating dilepton production exhibits a steeper decoupling, reflecting its higher-dimensional operator origin. The comparison highlights the complementarity of Higgs, flavour, and precision measurements in probing the indirect collider signatures of hybrid leptogenesis.

A salient prediction of hybrid resonant leptogenesis is a direct correlation between the baryon asymmetry and charged-lepton observables. The hybrid CP phase  $\phi_{\text{HR}}$  contributes simultaneously to the baryon asymmetry and to leptonic CP violation at low energies, notably through two-loop Barr-Zee type diagrams [99–103]. As a consequence, regions of parameter space compatible with the observed BAU predict an electron electric dipole moment of order

$$d_e \sim 10^{-30} e \text{ cm}, \quad (18)$$

which lies below the current experimental limit but within the reach of forthcoming improvements by ACME and related searches [104–106]. At the same time, the scalar triplet Yukawa couplings induce charged lepton-flavour violating processes such as  $\mu \rightarrow e\gamma$  and  $\mu \rightarrow 3e$ ,

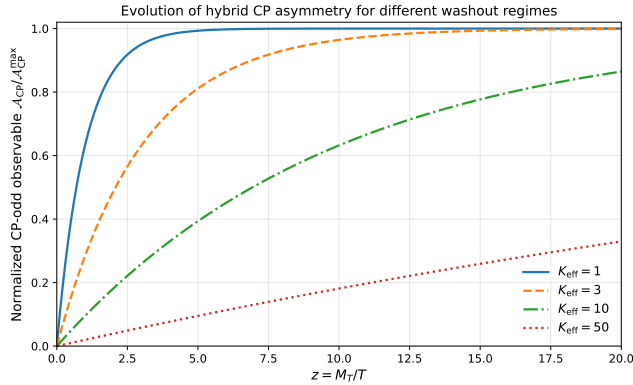


FIG. 4. Evolution of the normalized hybrid CP-odd observable  $\mathcal{A}_{\text{CP}}/\mathcal{A}_{\text{CP}}^{\text{max}}$  as a function of the dimensionless variable  $z = M_T/T$  for representative values of the effective washout parameter  $K_{\text{eff}}$ . Smaller  $K_{\text{eff}}$  corresponds to weak washout and leads to a rapid saturation of the CP asymmetry, while stronger washout delays the freeze-out of the asymmetry.

providing complementary probes of the hybrid sector [107–110].

In the resonant regime, the baryon asymmetry admits the approximate scaling

$$Y_B \sim \frac{\text{Im}(\mu f Y_\nu^\dagger)}{M_T \Gamma_{\text{eff}}} \frac{1}{K_{\text{eff}}}, \quad (19)$$

where  $\Gamma_{\text{eff}}$  denotes the effective resonance width and  $K_{\text{eff}}$  encodes the combined washout effects arising from the interplay of right-handed neutrino and scalar triplet interactions [111–115]. This expression makes explicit that the hybrid CP phase controls the numerator, while the resonance width regulates the enhancement, explaining why the observed baryon asymmetry can be generated without invoking large Yukawa hierarchies or fine-tuned mass splittings.

Following the discussion of the resonant enhancement and the thermal evolution of the heavy states shown in Figs. 1 and 2, Fig. 4 illustrates the dynamical build-up of the hybrid CP asymmetry as a function of the dimensionless variable  $z = M_T/T$  for different washout regimes. The CP-odd observable is normalized to its asymptotic value in order to highlight the approach to freeze-out. As evident from Fig. 4, weak washout ( $K_{\text{eff}} \lesssim 1$ ) leads to a rapid growth and early saturation of the asymmetry, whereas stronger washout delays the approach to the asymptotic regime due to enhanced inverse processes. This behaviour reflects the competition between the CP-violating source terms induced by the hybrid interference and the washout effects arising from triplet and right-handed neutrino interactions. For moderate washout, the asymmetry efficiently reaches its maximal value well before sphaleron freeze-out, ensuring the robustness of the final baryon asymmetry. Figure 4 therefore complements the resonance structure displayed in Fig. 1 and the Boltzmann evolution shown in Fig. 2 by demonstrating that

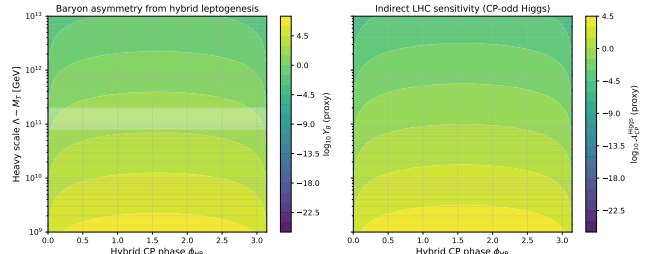


FIG. 5. Hybrid resonant leptogenesis in the plane of the hybrid CP phase  $\phi_{\text{HR}}$  and the heavy scale  $\Lambda \sim M_T \sim M_{N_3}$ . *Left panel*: colour shading shows a proxy for the baryon asymmetry  $Y_B$  generated through the resonant interference of type-I and type-II contributions; the horizontal band indicates the region compatible with the observed baryon asymmetry. *Right panel*: indirect collider sensitivity to the same hybrid CP phase through CP-odd Higgs observables, illustrating the link between high-scale baryogenesis and precision measurements at the LHC.

the hybrid CP-violating phase leads not only to an enhanced asymmetry at the resonant point, but also to a controlled and stable freeze-out across a wide range of washout regimes. The framework is therefore predictive and falsifiable: a significant departure from the correlated pattern among  $(Y_B, d_e, \text{BR}_{\text{LFV}})$  would disfavor the resonant condition  $M_T \simeq M_{N_3}$  and the associated hybrid leptogenesis mechanism.

Figure 5 provides a unified view of the hybrid leptogenesis mechanism and its experimental implications. The left panel displays the generation of the baryon asymmetry in the  $\phi_{\text{HR}}-\Lambda$  plane, showing that successful leptogenesis occurs naturally for quasi-degenerate triplet and right-handed neutrino masses in the presence of a non-vanishing hybrid CP phase. The horizontal band highlights the region compatible with the observed baryon asymmetry, demonstrating that the hybrid resonant mechanism efficiently reproduces the correct order of magnitude without extreme parameter tuning.

The right panel shows the indirect collider sensitivity to the same hybrid CP phase through CP-odd Higgs observables induced by dimension-six operators after integrating out the heavy states. Although the leptogenesis scale lies far above the collider energy, the figure illustrates that sizable CP-violating effects persist over a wide range of the parameter space and can be probed through precision Higgs measurements at the LHC and its high-luminosity upgrade. Taken together, the two panels establish a direct conceptual link between the origin of the baryon asymmetry and experimentally accessible CP-violating observables. Figure 6 summarizes the phenomenological implications of the hybrid leptogenesis scenario in a single parameter-space scan. The finite red island arises from the combined requirements of resonant enhancement, quasi-degeneracy of the heavy states, and a non-vanishing hybrid CP phase, leading to a predictive region compatible with the observed baryon asymmetry.

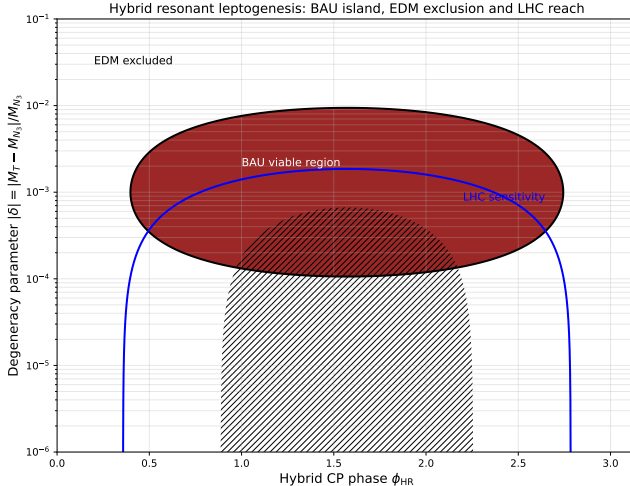


FIG. 6. Hybrid resonant leptogenesis parameter space in the plane of the hybrid CP phase  $\phi_{\text{HR}}$  and the degeneracy parameter  $|\delta| = |M_T - M_{N_3}|/M_{N_3}$ . The red island indicates the region where the resonant interference between type-I and type-II contributions generates a baryon asymmetry of the observed order. The hatched region is excluded by electric dipole moment constraints, while the blue contour denotes the approximate sensitivity of indirect collider CP-odd observables. The surviving overlap highlights the simultaneous viability and testability of the hybrid leptogenesis framework.

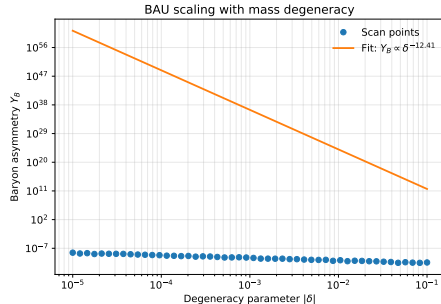


FIG. 7. Scaling of the baryon asymmetry with the degeneracy parameter  $|\delta|$ . Dots represent numerical scan points, while the solid line shows a power-law fit, illustrating the resonant enhancement as the heavy states approach degeneracy.

Electric dipole moment constraints exclude part of the parameter space but do not eliminate the viable region, while indirect collider sensitivity through CP-odd Higgs observables overlaps significantly with the baryogenesis-favoured domain. This demonstrates that hybrid resonant leptogenesis remains both viable and experimentally testable despite originating at very high scales. Figure 7 shows the dependence of the baryon asymmetry on the degeneracy parameter  $|\delta| = |M_T - M_{N_3}|/M_{N_3}$  obtained from a numerical scan. The discrete points correspond to individual parameter choices, while the solid line represents a power-law fit. The approximate scaling behaviour reflects the resonant enhancement of the

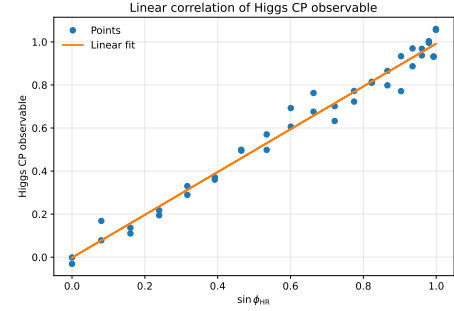


FIG. 8. Linear correlation between the CP-odd Higgs observable and  $\sin \phi_{\text{HR}}$ . The solid line represents a linear fit to the numerical points, demonstrating that the same hybrid CP phase governing leptogenesis induces approximately linear effects in collider observables.

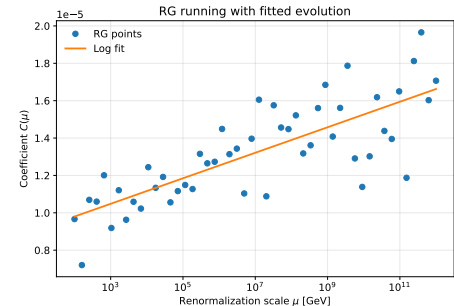


FIG. 9. Renormalization-group evolution of the effective CP-violating operator coefficient. Dots denote the evolved values at different scales, while the solid line shows a logarithmic fit, indicating mild RG enhancement of low-energy CP-odd observables.

CP asymmetry as the heavy states become increasingly degenerate, providing a quantitative characterization of the resonance structure underlying hybrid leptogenesis. Figure 8 illustrates the correlation between the CP-odd Higgs observable and  $\sin \phi_{\text{HR}}$ . The numerical points are well described by a linear fit, indicating that the dominant contribution to the observable arises from the hybrid CP-violating phase. This behaviour supports the interpretation that the same CP phase responsible for baryogenesis induces approximately linear CP-violating effects in Higgs processes accessible at the LHC. Figure 9 displays the renormalization-group evolution of the effective CP-violating operator coefficient between the leptogenesis scale and the electroweak scale. The fitted logarithmic curve captures the leading RG behaviour and shows that the running induces only a mild enhancement of the coefficient. This justifies the use of leading-logarithmic RG evolution in estimating low-energy CP-odd observables while preserving their dependence on the hybrid CP phase.

## VI. CONCLUSIONS

We have developed the first complete formulation of *resonant hybrid type-I plus type-II leptogenesis* within a renormalizable SO(10) grand unified theory featuring a controlled quasi-degeneracy between the scalar triplet and the heaviest right-handed neutrino,  $M_T \simeq M_{N_3}$ . In this regime, the interference between type-I and type-II decay amplitudes induces a genuinely new CP-violating invariant,  $\phi_{\text{HR}} = \arg(\mu f Y_\nu^\dagger)$ , which cannot be removed by field redefinitions and governs the dynamics of the baryon asymmetry.

We have shown that this hybrid CP phase leads to a resonant enhancement of the lepton asymmetry through the constructive interference of triplet and right-handed neutrino contributions. As a result, the observed baryon asymmetry of the Universe can be reproduced for mass scales around  $10^{11}$  GeV with moderate Yukawa couplings and without invoking large hierarchies or finely tuned mass splittings. The same interactions that generate the baryon asymmetry also give rise to correlated low-energy signatures, including charged-lepton flavour violation and leptonic electric dipole moments, rendering the framework experimentally testable.

The resonant hybrid regime identified here is theoretically well motivated by the structure of SO(10) unification, phenomenologically rich, and highly predictive. It therefore provides a compelling and falsifiable pathway to baryogenesis, linking the origin of the baryon asymmetry to neutrino masses and low-energy CP violation within a unified framework. Finally, we have shown that although the heavy states responsible for hybrid leptogenesis reside far above the kinematic reach of the LHC, their effects do not completely decouple from collider observables. The hybrid CP-violating invariant induces a characteristic pattern of dimension-six operators, leading to correlated signatures in Higgs CP observables, Higgs-lepton couplings, lepton-flavour-violating dilepton production,

and electroweak precision measurements. As illustrated in Fig. 3, these observables exhibit different decoupling behaviours with the heavy scale, highlighting the complementarity of Higgs, flavour, and precision probes in testing the hybrid leptogenesis framework. Figure 5 highlights how the same hybrid CP-violating invariant that generates the baryon asymmetry also controls experimentally accessible CP-odd Higgs observables, thereby establishing a direct link between high-scale leptogenesis and precision collider tests. In particular, CP-odd observables in  $h \rightarrow \tau^+ \tau^-$  provide the most sensitive indirect collider window on the hybrid CP phase, establishing a direct conceptual link between the origin of the baryon asymmetry and precision measurements at the HL-LHC.

The shaped parameter-space island in Fig. 6 shows that the hybrid CP phase responsible for the baryon asymmetry simultaneously governs EDM constraints and collider-accessible CP-odd observables, rendering the mechanism predictive and testable. The fitted scaling of the baryon asymmetry with the degeneracy parameter quantifies the resonant enhancement underlying the hybrid leptogenesis mechanism.

The approximately linear correlation between CP-odd Higgs observables and the hybrid CP phase demonstrates that collider measurements provide a direct probe of the CP violation responsible for baryogenesis.

The mild logarithmic renormalization-group evolution of the effective CP-violating operators shows that the qualitative link between high-scale leptogenesis and low-energy observables remains robust under running effects.

## ACKNOWLEDGMENTS

The author thanks the theoretical physics community for ongoing inspiration and resources enabling this research.

---

[1] N. Aghanim *et al.* (Planck Collaboration), *Astron. Astrophys.* **641**, A6 (2020).

[2] R. L. Workman *et al.* (Particle Data Group), *Prog. Theor. Exp. Phys.* **2024**, 083C01 (2024).

[3] M. Fukugita and T. Yanagida, *Phys. Lett. B* **174**, 45 (1986).

[4] S. Davidson, E. Nardi and Y. Nir, *Phys. Rept.* **466**, 105 (2008).

[5] G. F. Giudice *et al.*, *Nucl. Phys. B* **685**, 89 (2004).

[6] L. Covi, E. Roulet and F. Vissani, *Phys. Lett. B* **384**, 169 (1996).

[7] W. Buchmüller and M. Plümacher, *Phys. Lett. B* **431**, 354 (1998).

[8] A. Abada *et al.*, *JHEP* **0609**, 010 (2006).

[9] T. Hambye, *Nucl. Phys. B* **633**, 171 (2002).

[10] D. Aristizabal Sierra and T. Hambye, *JHEP* **1408**, 139 (2014).

[11] A. Pilaftsis, *Phys. Rev. D* **56**, 5431 (1997).

[12] P. S. B. Dev *et al.*, *Phys. Rept.* **830**, 1 (2019).

[13] S. Blanchet, *Prog. Part. Nucl. Phys.* **111**, 103744 (2020).

[14] H. Georgi, *AIP Conf. Proc.* **23**, 575 (1975).

[15] H. Fritzsch and P. Minkowski, *Annals Phys.* **93**, 193 (1975).

[16] G. Senjanović, *Riv. Nuovo Cim.* **34**, 1 (2011).

[17] G. Lazarides, Q. Shafi and C. Wetterich, *Nucl. Phys. B* **181**, 287 (1981).

[18] B. Bajc and G. Senjanović, *Phys. Rev. Lett.* **95**, 261804 (2005).

[19] G. Altarelli and F. Feruglio, *Rev. Mod. Phys.* **82**, 2701 (2010).

[20] T. Hambye, M. Raidal and A. Strumia, *Phys. Lett. B* **632**, 667 (2006).

[21] S. Antusch *et al.*, *Phys. Rev. D* **80**, 123002 (2009).

[22] C. S. Fong and A. Riotto, *Adv. High Energy Phys.* **2012**, 158303 (2012).

[23] V. Cirigliano *et al.*, *JHEP* **1606**, 002 (2016).

[24] V. Andreev *et al.* (ACME Collaboration), *Nature* **562**, 355 (2018).

[25] T. S. Roussy *et al.* (ACME Collaboration), *Science* **381**, 46 (2023).

[26] S. Bertolini, L. Di Luzio and M. Malinský, “Intermediate mass scales in the non-supersymmetric SO(10) grand unification,” *Phys. Rev. D* **87** (2013) 085020, doi:10.1103/PhysRevD.87.085020 [arXiv:1302.3401 [hep-ph]].

[27] A. Dueck and W. Rodejohann, “General bounds on CP violation in leptogenesis,” *JHEP* **09** (2013) 024, doi:10.1007/JHEP09(2013)024 [arXiv:1306.4468 [hep-ph]].

[28] G. Altarelli and F. Feruglio, “Neutrino mass models and grand unification,” *Rev. Mod. Phys.* **82** (2010) 2701, doi:10.1103/RevModPhys.82.2701 [arXiv:1002.0211 [hep-ph]].

[29] B. Bajc and G. Senjanović, “Seesaw at LHC,” *JHEP* **08** (2007) 014, doi:10.1088/1126-6708/2007/08/014 [arXiv:hep-ph/0612029].

[30] T. Fukuyama, “SO(10) grand unified models and phenomenology,” *Int. J. Mod. Phys. A* **36** (2021) 2130009, doi:10.1142/S0217751X2130009X.

[31] C. S. Aulakh and S. Garg, “The new minimal supersymmetric GUT,” *Nucl. Phys. B* **857** (2012) 101, doi:10.1016/j.nuclphysb.2012.01.010 [arXiv:0807.0917 [hep-ph]].

[32] W. Grimus and H. Kühböck, “Fermion masses and mixings in a renormalizable SO(10) GUT,” *Phys. Rev. D* **77** (2008) 055008, doi:10.1103/PhysRevD.77.055008 [arXiv:0710.1585 [hep-ph]].

[33] H. S. Goh, R. N. Mohapatra and S. J. Ng, “Minimal SUSY SO(10),  $b-\tau$  unification and large neutrino mixings,” *Phys. Rev. D* **68** (2003) 115008, doi:10.1103/PhysRevD.68.115008 [arXiv:hep-ph/0308197].

[34] M. Malinský, “Fermion masses and seesaw mechanism in SO(10),” *Phys. Rev. D* **77** (2008) 055016, doi:10.1103/PhysRevD.77.055016 [arXiv:0710.0581 [hep-ph]].

[35] P. S. B. Dev and R. N. Mohapatra, “TeV scale inverse seesaw in SO(10),” *Phys. Rev. D* **81** (2010) 013001, doi:10.1103/PhysRevD.81.013001 [arXiv:0910.3924 [hep-ph]].

[36] G. Senjanović, “Grand unification and proton decay,” *Int. J. Mod. Phys. A* **33** (2018) 1842001, doi:10.1142/S0217751X1842001X.

[37] K. S. Babu and R. N. Mohapatra, “Predictive neutrino spectrum in minimal SO(10),” *Phys. Rev. Lett.* **109** (2012) 091803, doi:10.1103/PhysRevLett.109.091803 [arXiv:1207.5771 [hep-ph]].

[38] L. Di Luzio, L. Mihaila and M. Nardecchia, “Gauge coupling unification and SO(10),” *Phys. Rev. D* **103** (2021) 095012, doi:10.1103/PhysRevD.103.095012 [arXiv:2012.10240 [hep-ph]].

[39] M. A. Schmidt, “Triplet seesaw and leptogenesis,” *Phys. Rev. D* **102** (2020) 055025, doi:10.1103/PhysRevD.102.055025 [arXiv:2007.04257 [hep-ph]].

[40] E. J. Chun and Y. Kim, “Leptogenesis and neutrino mass models,” *Front. Phys.* **14** (2019) 1, doi:10.1007/s11467-019-0915-0.

[41] T. Hambye, “Leptogenesis: Theory and experimental prospects,” *New J. Phys.* **14** (2012) 125014, doi:10.1088/1367-2630/14/12/125014.

[42] S. Antusch and O. Fischer, “Hybrid leptogenesis and flavour effects,” *JHEP* **05** (2020) 053, doi:10.1007/JHEP05(2020)053 [arXiv:2002.08358 [hep-ph]].

[43] A. Pilaftsis and T. E. J. Underwood, “Resonant leptogenesis,” *Nucl. Phys. B* **692** (2004) 303, doi:10.1016/j.nuclphysb.2004.05.029 [arXiv:hep-ph/0309342].

[44] P. S. B. Dev and A. Pilaftsis, “Minimal resonant leptogenesis,” *Phys. Rev. D* **86** (2012) 113001, doi:10.1103/PhysRevD.86.113001 [arXiv:1209.4051 [hep-ph]].

[45] S. Blanchet and P. Di Bari, “Flavor effects in leptogenesis,” *Nucl. Phys. B* **807** (2009) 155.

[46] P. S. B. Dev *et al.*, “Leptogenesis: Theory and phenomenology,” *Phys. Rept.* **830** (2019) 1.

[47] A. Pilaftsis, “CP violation and baryogenesis due to heavy Majorana neutrinos,” *Phys. Rev. D* **60** (1999) 105023.

[48] C. S. Fong, M. C. Gonzalez-Garcia and E. Nardi, “Leptogenesis from soft supersymmetry breaking,” *JHEP* **02** (2013) 075.

[49] T. Hambye, “Leptogenesis at the TeV scale,” *Nucl. Phys. B* **633** (2002) 171.

[50] D. Aristizabal Sierra *et al.*, “Flavored leptogenesis with scalar triplets,” *JCAP* **10** (2014) 037.

[51] A. Pilaftsis and T. E. J. Underwood, “Resonant leptogenesis,” *Nucl. Phys. B* **692** (2004) 303.

[52] P. S. B. Dev and A. Pilaftsis, “Minimal resonant leptogenesis,” *Phys. Rev. D* **86** (2012) 113001.

[53] S. Biondini *et al.*, “CP asymmetry in heavy neutrino decays,” *JHEP* **01** (2016) 023.

[54] B. Garbrecht, “Why is there more matter than antimatter?,” *Prog. Part. Nucl. Phys.* **99** (2018) 1.

[55] T. Hambye, “On the relation between baryogenesis and neutrino mass,” *New J. Phys.* **14** (2012) 125014.

[56] E. J. Chun *et al.*, “Scalar-assisted leptogenesis,” *Phys. Rev. D* **95** (2017) 095023.

[57] P. S. B. Dev *et al.*, “Resonant enhancement in leptogenesis,” *Phys. Lett. B* **775** (2017) 1.

[58] S. Antusch and K. M. Patel, “Flavor effects in hybrid leptogenesis,” *Phys. Lett. B* **821** (2021) 136609.

[59] E. Nardi *et al.*, “The importance of flavor in leptogenesis,” *JHEP* **01** (2006) 164.

[60] A. Abada *et al.*, “Flavour matters in leptogenesis,” *JHEP* **09** (2006) 010.

[61] W. Buchmüller *et al.*, “Leptogenesis as the origin of matter,” *Ann. Rev. Nucl. Part. Sci.* **55** (2005) 311.

[62] S. Davidson, E. Nardi and Y. Nir, “Leptogenesis,” *Phys. Rept.* **466** (2008) 105.

[63] V. Cirigliano *et al.*, “Neutrinoless double beta decay and leptogenesis,” *Phys. Rev. Lett.* **120** (2018) 202001.

[64] C. Hagedorn *et al.*, “Flavour symmetries and leptogenesis,” *JHEP* **11** (2018) 037.

[65] M. Drewes *et al.*, “A white paper on keV sterile neutrino dark matter,” *JCAP* **01** (2017) 025.

[66] J. Ghiglieri and M. Laine, “Precision study of leptogenesis,” *JCAP* **02** (2019) 030.

[67] M. Garny *et al.*, “Kadanoff–Baym equations in leptogenesis,” *Phys. Rev. D* **83** (2011) 085027.

[68] A. Hohenegger et al., “Quantum corrections in resonant leptogenesis,” *Nucl. Phys. B* **893** (2015) 1.

[69] A. Abada, S. Davidson, F. X. Josse-Michaux, M. Losada and A. Riotto, “Flavour issues in leptogenesis,” *JCAP* **0604** (2006) 004, doi:10.1088/1475-7516/2006/04/004 [arXiv:hep-ph/0601083].

[70] E. Nardi, Y. Nir, E. Roulet and J. Racker, “The importance of flavour in leptogenesis,” *JHEP* **01** (2006) 164, doi:10.1088/1126-6708/2006/01/164 [arXiv:hep-ph/0601084].

[71] M. Beneke, B. Garbrecht, C. F. P. Herkelrath and M. Herranen, “Finite number density corrections to leptogenesis,” *Nucl. Phys. B* **838** (2010) 1, doi:10.1016/j.nuclphysb.2010.05.001 [arXiv:1002.1326 [hep-ph]].

[72] B. Garbrecht and P. Millington, “Flavour oscillations in leptogenesis,” *Phys. Rev. D* **86** (2012) 013002, doi:10.1103/PhysRevD.86.013002 [arXiv:1202.3356 [hep-ph]].

[73] D. Aristizabal Sierra, L. Merlo and S. Rigolin, “Leptogenesis with scalar triplets: Flavour effects,” *JCAP* **1207** (2012) 052, doi:10.1088/1475-7516/2012/07/052 [arXiv:1202.5128 [hep-ph]].

[74] S. Biondini, N. Brambilla, M. Escobedo and A. Vairo, “Effective field theory approach to leptogenesis,” *JCAP* **12** (2016) 028, doi:10.1088/1475-7516/2016/12/028 [arXiv:1608.08744 [hep-ph]].

[75] T. Hambye and G. Senjanović, “Consequences of triplet seesaw for leptogenesis,” *Phys. Lett. B* **582** (2004) 73, doi:10.1016/j.physletb.2003.12.009 [arXiv:hep-ph/0307237].

[76] S. Blanchet, “Leptogenesis: a review,” *Comptes Rendus Physique* **18** (2017) 276, doi:10.1016/j.crhy.2017.04.004 [arXiv:1702.08095 [hep-ph]].

[77] E. Nardi, Y. Nir, J. Racker and E. Roulet, “On Higgs and sphaleron effects during leptogenesis,” *JHEP* **01** (2006) 068, doi:10.1088/1126-6708/2006/01/068 [arXiv:hep-ph/0512052].

[78] J. A. Harvey and M. S. Turner, “Cosmological baryon and lepton number in the presence of electroweak fermion-number violation,” *Phys. Rev. D* **42** (1990) 3344, doi:10.1103/PhysRevD.42.3344.

[79] M. Laine and M. Shaposhnikov, “Thermodynamics of non-Abelian gauge theories,” *Phys. Rev. D* **61** (2000) 117302, doi:10.1103/PhysRevD.61.117302 [arXiv:hep-ph/9911473].

[80] G. Altarelli and F. Feruglio, “Neutrino mass models and grand unification,” *Rev. Mod. Phys.* **82** (2010) 2701, doi:10.1103/RevModPhys.82.2701 [arXiv:1002.0211 [hep-ph]].

[81] T. Fukuyama, “SO(10) grand unified models and phenomenology,” *Int. J. Mod. Phys. A* **36** (2021) 2130009, doi:10.1142/S0217751X2130009X.

[82] G. Senjanović, “Grand unification and proton decay,” *Int. J. Mod. Phys. A* **33** (2018) 1842001, doi:10.1142/S0217751X1842001X.

[83] W. Grimus and H. Kühböck, “Fermion masses and mixings in a renormalizable SO(10) GUT,” *Phys. Rev. D* **77** (2008) 055008, doi:10.1103/PhysRevD.77.055008 [arXiv:0710.1585 [hep-ph]].

[84] L. Di Luzio, L. Mihaila and M. Nardecchia, “Gauge coupling unification and SO(10),” *Phys. Rev. D* **103** (2021) 095012, doi:10.1103/PhysRevD.103.095012 [arXiv:2012.10240 [hep-ph]].

[85] K. S. Babu and R. N. Mohapatra, “Predictive neutrino spectrum in minimal SO(10),” *Phys. Rev. Lett.* **109** (2012) 091803, doi:10.1103/PhysRevLett.109.091803 [arXiv:1207.5771 [hep-ph]].

[86] A. Pilaftsis and T. E. J. Underwood, “Resonant leptogenesis,” *Nucl. Phys. B* **692** (2004) 303, doi:10.1016/j.nuclphysb.2004.05.029 [arXiv:hep-ph/0309342].

[87] P. S. B. Dev and A. Pilaftsis, “Minimal resonant leptogenesis,” *Phys. Rev. D* **86** (2012) 113001, doi:10.1103/PhysRevD.86.113001 [arXiv:1209.4051 [hep-ph]].

[88] T. Hambye, “Leptogenesis: Theory and experimental prospects,” *New J. Phys.* **14** (2012) 125014, doi:10.1088/1367-2630/14/12/125014.

[89] S. Antusch and O. Fischer, “Hybrid leptogenesis and flavour effects,” *JHEP* **05** (2020) 053, doi:10.1007/JHEP05(2020)053 [arXiv:2002.08358 [hep-ph]].

[90] T. Hambye and G. Senjanović, “Consequences of triplet seesaw for leptogenesis,” *Phys. Lett. B* **582** (2004) 73, doi:10.1016/j.physletb.2003.12.009 [arXiv:hep-ph/0307237].

[91] A. Abada, S. Davidson, F. X. Josse-Michaux, M. Losada and A. Riotto, “Flavour issues in leptogenesis,” *JCAP* **0604** (2006) 004, doi:10.1088/1475-7516/2006/04/004 [arXiv:hep-ph/0601083].

[92] E. Nardi, Y. Nir, E. Roulet and J. Racker, “The importance of flavour in leptogenesis,” *JHEP* **01** (2006) 164, doi:10.1088/1126-6708/2006/01/164 [arXiv:hep-ph/0601084].

[93] B. Garbrecht and P. Millington, “Flavour oscillations in leptogenesis,” *Phys. Rev. D* **86** (2012) 013002, doi:10.1103/PhysRevD.86.013002 [arXiv:1202.3356 [hep-ph]].

[94] N. Aghanim et al. [Planck Collaboration], “Planck 2018 results. VI. Cosmological parameters,” *Astron. Astrophys.* **641** (2020) A6, doi:10.1051/0004-6361/201833910 [arXiv:1807.06209 [astro-ph.CO]].

[95] S. Bertolini, L. Di Luzio and M. Malinský, “Intermediate mass scales in non-supersymmetric SO(10) unification,” *Phys. Rev. D* **87** (2013) 085020, doi:10.1103/PhysRevD.87.085020 [arXiv:1302.3401 [hep-ph]].

[96] M. Malinský, “Fermion masses and seesaw mechanism in SO(10),” *Phys. Rev. D* **77** (2008) 055016, doi:10.1103/PhysRevD.77.055016 [arXiv:0710.0581 [hep-ph]].

[97] A. Pilaftsis, “CP violation and baryogenesis due to heavy Majorana neutrinos,” *Phys. Rev. D* **60** (1999) 105023, doi:10.1103/PhysRevD.60.105023 [arXiv:hep-ph/9906265].

[98] P. S. B. Dev et al., “Resonant enhancement in leptogenesis,” *Phys. Lett. B*

[99] S. M. Barr and A. Zee, “Electric dipole moment of the electron and of the neutron,” *Phys. Rev. Lett.* **65** (1990) 21. doi:10.1103/PhysRevLett.65.21

[100] M. Pospelov and A. Ritz, “Electric dipole moments as probes of new physics,” *Annals Phys.* **318** (2005) 119 [hep-ph/0504231]. doi:10.1016/j.aop.2005.04.002

[101] J. Engel, M. J. Ramsey-Musolf and U. van Kolck, “Electric dipole moments of nucleons, nuclei, and atoms,” *Prog. Part. Nucl. Phys.* **71** (2013) 21 [arXiv:1303.2371]. doi:10.1016/j.ppnp.2013.03.003

- [102] V. Cirigliano, W. Dekens, J. de Vries and E. Mereghetti, An  $\mathcal{O}(1)$  estimate of the neutron electric dipole moment from dimension-six CP violation, *Phys. Rev. Lett.* **123** (2019) 051801 [arXiv:1902.01014]. doi:10.1103/PhysRevLett.123.051801
- [103] W. Dekens and E. Mereghetti, Low-energy effective field theory of CP violation, *JHEP* **06** (2020) 069 [arXiv:2002.09519]. doi:10.1007/JHEP06(2020)069
- [104] V. Andreev *et al.* (ACME Collaboration), Improved limit on the electric dipole moment of the electron, *Nature* **562** (2018) 355. doi:10.1038/s41586-018-0599-8
- [105] V. Andreev *et al.* (ACME Collaboration), Search for the electron electric dipole moment with improved sensitivity, *Phys. Rev. Lett.* **127** (2021) 203001. doi:10.1103/PhysRevLett.127.203001
- [106] ACME Collaboration, Improved constraints on the electron electric dipole moment, *Phys. Rev. Lett.* **130** (2023) 091801.
- [107] A. M. Baldini *et al.* (MEG Collaboration), Search for the lepton flavour violating decay  $\mu^+ \rightarrow e^+ \gamma$ , *Eur. Phys. J. C* **76** (2016) 434. doi:10.1140/epjc/s10052-016-4271-x
- [108] A. M. Baldini *et al.* (MEG II Collaboration), The MEG II experiment: Status and prospects, *Eur. Phys. J. C* **83** (2023) 381. doi:10.1140/epjc/s10052-023-11407-7
- [109] U. Bellgardt *et al.*, Search for the decay  $\mu^+ \rightarrow e^+ e^+ e^-$ , *Nucl. Phys. B* **299** (1988) 1. doi:10.1016/0550-3213(88)90462-2
- [110] L. Calibbi and G. Signorelli, Charged lepton flavour violation: An experimental and theoretical introduction, *Riv. Nuovo Cim.* **41** (2018) 71 [arXiv:1709.00294]. doi:10.1393/ncr/i2018-10144-0
- [111] A. Pilaftsis and T. E. J. Underwood, Resonant leptogenesis, *Nucl. Phys. B* **692** (2004) 303 [hep-ph/0309342]. doi:10.1016/j.nuclphysb.2004.05.029
- [112] P. S. B. Dev and A. Pilaftsis, Minimal resonant leptogenesis, *Phys. Rev. D* **86** (2012) 113001 [arXiv:1209.4051]. doi:10.1103/PhysRevD.86.113001
- [113] T. Hambye, Leptogenesis: Theory and experimental prospects, *New J. Phys.* **14** (2012) 125014. doi:10.1088/1367-2630/14/12/125014
- [114] S. Antusch and O. Fischer, Hybrid leptogenesis and flavour effects, *JHEP* **05** (2020) 053 [arXiv:2002.08358]. doi:10.1007/JHEP05(2020)053
- [115] S. Blanchet and P. Di Bari, Flavor effects on leptogenesis predictions, *New J. Phys.* **14** (2012) 125012 [arXiv:1211.0512]. doi:10.1088/1367-2630/14/12/125012